J. Math. Biol. (2007) 54:797–813
DOI 10.1007/s00285-007-0071-0

Mathematical Biology

Soliton behaviour in a bistable reaction diffusion model

C. Varea · D. Hernández · R. A. Barrio

Received: 19 August 2006 / Revised: 13 November 2006 / Published online: 15 February 2007

Abstract We analyze a generic reaction-diffusion model that contains the important features of Turing systems and that has been extensively used in the past to model biological interesting patterns. This model presents various fixed points. Analysis of this model has been made in the past only in the case when there is only a single fixed point, and a phase diagram of all the possible instabilities shows that there is a place where a Turing-Hopf bifurcation occurs producing oscillating Turing patterns. In here we focus on the interesting situation of having several fixed points, particularly when one unstable point is in between two equally stable points. We show that the solutions of this bistable system are traveling front waves, or solitons. The predictions and results are tested by performing extensive numerical calculations in one and two dimensions. The dynamics of these solitons is governed by a well defined spatial scale, and collisions and interactions between solitons depend on this scale. In certain regions of parameter space the wave fronts can be stationary, forming a pattern resembling spatial chaos. The patterns in two dimensions are particularly interesting because they can present a coherent dynamics with pseudo spiral rotations that simulate the myocardial beat quite closely. We show that our simple model can produce complicated spatial patterns with many different properties, and could be used in applications in many different fields.

Keywords Solitons · Reaction-diffusion models · Pattern formation

C. Varea (✉) · D. Hernández · R. A. Barrio
Instituto de Física, Universidad Nacional Autónoma de México (UNAM),
Apartado Postal 20-364, 01000 México, D.F., México
e-mail: varea@fisica.unam.mx

R. A. Barrio
e-mail: barrio@fisica.unam.mx

Mathematics Subject Classification (2000) 35K57 · 74J35

1 Introduction

There has been a renewed interest in studying systems that present a diffusion driven instability. This mechanism provides an understandable and easy way of producing non-oscillating robust spatial patterns that can be seen in many complex systems, particularly in biology, embryology, and of course, chemistry [6]. The original idea that Alan Turing [16] envisaged as to explain many facts in morphogenesis by this kind of process has been far off being proven, due mainly to two facts, first, the difficulty to find and recognize the morphogens in real systems, and second, the simplicity of the patterns that are generally obtained with these systems. It is found that the Turing instability produces simple striped patterns, or an hexagonal array of spots, or a combination of the two. The former being enhanced by a cubic non-linearity, and the spots by quadratic terms [3].

There have been efforts to construct complicated patterns with Turing systems, either by using special boundary conditions [1], curved and growing domains [14], or by coupling two Turing systems linearly [17] or non-linearly [1]. All of these show that the non-linear dynamics and the pattern selection processes in Turing systems are more complicated than expected and that at present there is much to be learned from them. It is the purpose of this paper to show that reaction-diffusion systems present an unsuspected richness of behaviors. We choose a generic reaction diffusion model put forward by us [3] and used extensively in the past to model various patterns found in biological systems, such as the coloring of marine fish [1], or the symmetry and form of sea urchin shells [2], and others [10]. The kinetics are constructed by assuming that there is a fixed point at the origin, and by expanding all the possible non-linear terms around it up to third order. Namely,

$$\begin{aligned} \frac{\partial u}{\partial t} &= \delta D \nabla^2 u + \alpha u(1 - r_1 v^2) + v(1 - r_2 u) \\ \frac{\partial v}{\partial t} &= \delta \nabla^2 v + v(\beta + \alpha r_1 u v) + u(\gamma + r_2 v), \end{aligned} \tag{1}$$

where, δ is a scaling factor, D is the ratio of diffusion coefficients of chemicals u and v. The parameters governing the kinetics are r_1, r_2, α, β and γ. The first two represent the strength of the cubic and quadratic non-linearities, respectively.

In all former applications this model has been used as a true Turing system meeting all the conditions for a Turing instability. Furthermore, it has been assumed that $\gamma = -\alpha$, which ensures that there is only one fixed point at the origin $(u, v) = (0, 0)$. A detailed analysis of the instability in this case has been made before [9] showing that beyond the region where a Turing instability appears, there is the possibility of having a "Turing-Hopf" bifurcation that produces spatial patterns oscillating in time.

Then, the question arises naturally of having more complicated behavior when one has more fixed points. When $\gamma \neq -\alpha$, two additional fixed points appear. Then, if these points are stable, one could have a situation analogous to a thermodynamic system driven to a spinodal decomposition situation, in which two phases coexist and evolve in time. This bistability situation is interesting, since there is the possibility of having wave front profiles between the regions where the two different stable phases meet. It is our purpose to investigate peculiar situations like this.

The paper is organized as follows: in the first section the model is presented and linear analysis around the fixed points when $\gamma \neq -\alpha$ is performed in zero dimensions (absence of diffusion). We then study a surface of the phase diagram, keeping only cubic terms, to situate the two fixed points symmetrically around zero. We concentrate on a particularly interesting region of this surface, where linear analysis in one dimension predicts equal stability of the two fixed points. We predict solutions on the form of traveling waves and study their properties analytically and numerically. Finally, we perform numerical calculations in two dimensions and show some interesting patterns. In the last section the results are discussed and the implications to applications are pointed out, together with a summary of the most important conclusions of this work.

2 The model

It is convenient to cast Eq. 1 in a convenient form,

$$\begin{aligned} \frac{\partial u}{\partial t} &= D\nabla^2 u + \eta(u + av - Cuv - uv^2) \\ \frac{\partial v}{\partial t} &= \nabla^2 v + \eta(bv + hu + Cuv + uv^2) \end{aligned} \tag{2}$$

where $a = 1/\alpha$, $b = \beta/\alpha$, $h = \gamma/\alpha$, $C = r_2/(\alpha\sqrt{r_1})$ and $\eta = L^2\alpha/\delta$. In this equation we have redefined the variables substituting $x \to Lx$, $t \to L^2/\delta T$, $u \to u/\sqrt{r_1}$ and $v \to v/\sqrt{r_1}$. This model has only one stationary state at $u = v = 0$ when $h = -1$. One can perform a linear stability analysis around this point in the usual way. A complete analysis of this situation, including a nonlinear analysis of the amplitude equations, has been published elsewhere [9].

The model of Eq. 2 has two other fixed points when $h \neq -1$, located at

$$v_0 = \frac{-C \pm \sqrt{C^2 - 4(h - b/g)}}{2} \tag{3}$$

and,

$$u_0 = -gv_0 \tag{4}$$

where $g = (a + b)/(1 + h)$.

In the absence of quadratic terms ($C = 0$), one has an interesting situation, with three singular points situated symmetrically around zero. Besides the point

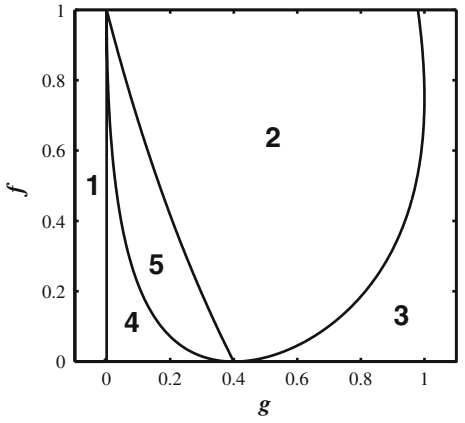

Fig. 1 Phase diagram of Eq. 2 in the absence of diffusion, when $C = 0, h = -2.5$. The character of the eigenvalues change in the different regions labeled by numbers. See text for explanation. The lines were calculated by the conditions extracted from the dispersion relation Eq. 5

$(u, v) = (0, 0)$, one has two symmetrical points at $v_0 = \pm\sqrt{b/g - h} = \pm\sqrt{f}$, and $u_0 = -gv_0$. This situation implies that one has the possibility of two equally stable phases, competing with each other. It is interesting to note that our model is not Hamiltonian, and even in the absence of quadratic terms, the model cannot be reduced to a form similar to the complex Landau-Ginzburg model, which has been extensively studied and applied in the past [15]. From now on we shall concentrate our attention to the case $C = 0$ and analyze the possible instabilities of the model by linearizing around the symmetric fixed points. In the absence of diffusion (zero dimensions), one gets the dispersion relation

$$\omega^2 - \omega X + Y = 0. \tag{5}$$

where $X = \eta[1-f+g(h-f)] = \mathrm{Tr(j)}$, and $Y = \eta^2 g[(h-f)(1-f)-(h+f)(1+f)]$ $= \mathrm{Det(j)}$, where j is the Jacobian matrix of the linearized kinetics.

If one fixes the value of h, one can examine the behavior of the eigenvalues $\omega_{1,2} = \sigma_{1,2} + i\tau$ of the linearized equations in the plane (g, f). If $Y = 0$ one of the roots is $\omega = 0$ and the other is real (observe that since $h \neq -1, \Rightarrow g = 0$). The condition $X = 0$ separates the region where σ changes sign. The discriminant condition $X^2 - 4Y = 0$ separates the regions of real and complex roots. These three conditions divide the (g, f) space in five regions.

In Fig. 1 we show these regions for $h = -2.5$:

In region 1, $\sigma_1 < 0, \sigma_2 > 0$ and $\tau = 0$, (saddle points).
In region 2, $\sigma_{1,2} < 0$ and $\tau \neq 0$, (oscillating stable points).
In region 3, $\sigma_{1,2} < 0$, and $\tau = 0$, (stable points).
In region 4, $\sigma_{1,2} > 0$ and $\tau = 0$, (both points are unstable).
In region 5, $\sigma_{1,2} > 0$ and $\tau \neq 0$, (oscillating unstable points).

We can analyze these results in more detail. In region 1 there are saddle points, therefore the trajectories that start in the vicinity of the fixed points first approach them, and then go away. As a result of the cubic reaction terms, there is a stable limit cycle that encompasses the two fixed points. The existence of

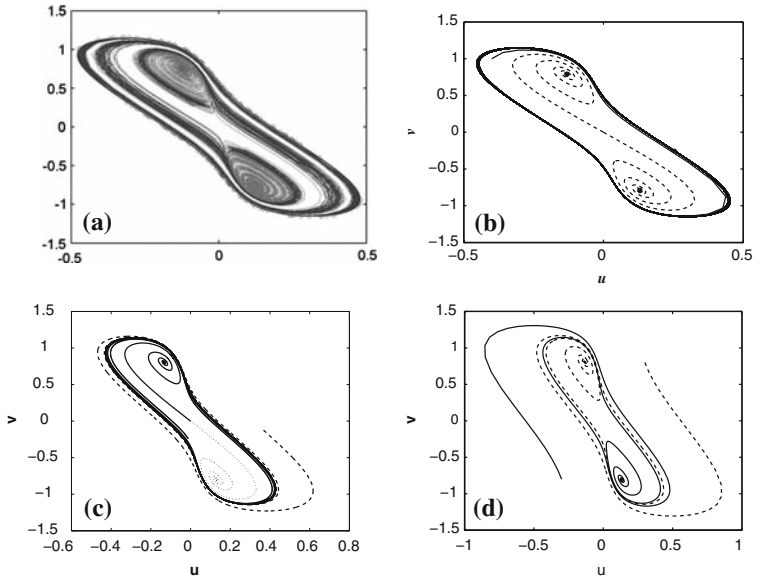

Fig. 2 **a** Phase portrait in region 2 but very near the border with region 5. Using $h = -2.5, g = 0.165$ the value at the border is $f_c = (1 + hg)/(g + 1) = 0.5043$. This figure was taken with $f = f_c + 0.07$. **b** same as **a** but $f = f_c + 0.12$. **c** same as **b** with $f = f_c + 0.14$. We found numerically that at this point the limit cycle appears for the last time, when one increases the value of f to $f_c + 0.15$ as in **d**, the limit cycle disappears

this limit cycle was corroborated by numerical calculations. In region 5 the fixed points are unstable, therefore the trajectories that start in their vicinity go away in an oscillating manner. There is a limit cycle also in this region. In region 2 the roots are both stable, but with an oscillatory contribution. Regions 4 and 3 are not relevant to our purposes, because the trajectories either diverge or converge to the fixed points. In region 3 there is the possibility of an instability driven by diffusion, producing stationary spatial Turing patterns.

In what follows we shall concentrate on region 2 in the vicinity of region 5. This region is suitable for our purposes, because one expects oscillating patterns that are equally stable around any of the two fixed points. In principle in this region there should not be a limit cycle. However, numerical calculations show that the limit cycle of region 5 persists in region 2 near the border between the two regions.

In order to investigate the behaviour of the system around the fixed points, we performed numerical calculations to obtain the phase portraits, using a simple Euler method.

In Fig. 2 we present a series of phase portraits starting very near the critical value of $f_c = (1 + hg)/(g + 1)$ that separates regions 2 and 5, maintaining $g = 0.165$ constant, and steadily going into region 2 far from the border. In Fig. 2a one observes two additional unstable limit cycles. These limit cycles separate a basin of attraction around the fixed points, and the basin of attraction for

the outer stable limit cycle in the figure, the gray trajectories end up at the fixed points, and the black ones join the stable limit cycle. Notice that the basin of attraction of the outer limit cycle contains the fixed point at the origin. In Fig. 2b we see that the basin of attraction of the fixed points increases and contains the origin. If one starts at the origin one ends up at one of the fixed points, as shown in the figure by the dashed trajectory. Far from the origin, one approaches the limit cycle. More into region 2 we observe that the stable limit cycle eventually disappears. In Fig. 2c we show the last limit cycle found numerically. Fig. 2d shows the simple picture expected for region 2.

It would be interesting to investigate in more detail the truly bistable situation when there are only two equally stable fixed points. In a model with a potential, one would simply expect a spinodal decomposition leading to Oswald ripening in the late stages of phase separation, with a characteristic length growing as a power law in time [4]. Our model does not admit a potential function for the kinetics, and the problem is fundamentally different. As we shall see, the phases are separated by a well defined scale, and the problem admits traveling wave front solutions, a feature that seems to be universal in many bistable non-linear systems.

2.1 Dynamics in one dimension

Let us examine the behavior of the model in one dimension. If we use appropriate parameters to be in region 2, we have the situation depicted in Fig. 2d, in which there are two symmetrical equally stable points and the point (0,0) is unstable. If we perform linear analysis around this central point, we can choose the parameters f, g, h, and η in order to produce a hyperbolic central fixed point. Then, in region 2 the other two fixed points are stable.

We can predict the existence of traveling wave fronts, an almost universally recognized feature of bistable reaction-diffusion systems [12]. We expect heteroclinic trajectories in phase space connecting the two stable fixed points with the central hyperbolic point. In order to illustrate the properties of traveling wave front solutions, we perform a linear analysis around the point (u_0, v_0), assuming that $u(x,t) = u(x - ct) = u(\gamma)$, and the same for $v(x,t)$. We start with Eq. 2 with $C = 0$, and substitute the solutions. We end up with two second order ordinary differential equations (ODE). These could be written as a set of four first order ODE by defining two fields, θ and ϕ. That is

$$\begin{aligned} \frac{du}{d\gamma} &= \theta, \\ \frac{d\theta}{d\gamma} &= -\tfrac{c}{D}\theta - F, \\ \frac{dv}{d\gamma} &= \phi, \\ \frac{d\phi}{d\gamma} &= -c\phi - G \end{aligned} \tag{6}$$

where $F = \frac{\eta}{D}(u + av - uv^2)$ and $G = \eta(bv + hu + uv^2)$. We define the Jacobian

$$\mathrm{J} = \begin{pmatrix} \partial F/\partial u & \partial F/\partial v \\ \partial G/\partial u & \partial G/\partial v \end{pmatrix} = \begin{pmatrix} \alpha_{11} & \alpha_{12} \\ \alpha_{21} & \alpha_{22} \end{pmatrix}. \tag{7}$$

The characteristic polynomial is

$$\lambda^4 + \mathrm{Tr}\mathrm{J}\lambda^2 + \mathrm{Det}\mathrm{J} + c\lambda\left[\left(1 + \frac{1}{D}\right)\lambda^2 + \frac{c}{D}\lambda + \frac{\alpha_{22}}{D} + \alpha_{11}\right] = 0 \tag{8}$$

The roots of Eq. 8 when $D = 1$ can be connected with our eigenvalue ω for zero dimensions, indeed

$$\lambda^2 + c\lambda + \omega = 0. \tag{9}$$

Observe that λ^{-1} is a distance that gives the decaying length of a fluctuation around the fixed point. Eq. 9 will be useful later on, when interpreting the numerical results.

The solution for $c = 0$ is

$$\lambda_{\pm}^2 = \frac{1}{2}\left(-\mathrm{Tr}\mathrm{J} \pm \sqrt{(\mathrm{Tr}\mathrm{J})^2 - 4\mathrm{Det}\mathrm{J}}\right), \tag{10}$$

and gives the heteroclinic trajectory connecting the two stable points, passing through the central unstable point. In this case the roots of Eq. 8 are of the form $\lambda = \pm\sigma_1 \pm i\tau_1$, that is, a single value of the real and imaginary parts appears. These solutions, which predict symmetric profiles of $u(x,t)$ and $v(x,t)$ should be unstable under small perturbations; the truly stable solutions predict asymmetric profiles traveling with velocity c. This can be easily understood by assuming that $u(x,t) = u(x - ct)$ and $v(x,t) = v(x - ct)$. Then

$$\begin{aligned} -c\frac{du}{dx} &= D\frac{d^2u}{dx^2} + DF \\ -c\frac{dv}{dx} &= \frac{d^2v}{dx^2} + G \end{aligned} \tag{11}$$

Adding these ODE and integrating, one gets

$$-c\int_{-\infty}^{\infty} d(u+v) = \eta(1+h)\int_{-\infty}^{\infty}(u+gv)dx + \int_{-\infty}^{\infty} d\left(\frac{d(Du+v)}{dx}\right). \tag{12}$$

The integral on the left hand side is just $2c(u_0 + v_0)$, the first integral on the right hand side is just a number that measures the asymmetry of the profiles, that is, if the area under the curves is equally negative than positive, this constant is zero, a situation known as the Maxwell condition. The last integral is zero because the slope of the profile at infinity is zero. Then the velocity of the front is directly proportional to the value of the first integral.

We can think of an infinite system with initial conditions such that in the left hand side one sets the u and v values to correspond to one of the stable points, and on the right hand side the initial concentrations correspond to the other stable point. Then one expects that somewhere there is a transition region between these two states. This kink in general could move or be stationary, according to Eq. 8. We are interested in studying the dynamics of this wave front. Observe that the exact shape of the kink is difficult to obtain. However, from the fact that the eigenvalues λ from Eq. 8 are always complex, the profile of the fronts approaches the fixed point in an oscillating way. The profile can be investigated by solving the equations numerically.

We performed a numerical calculation in a lattice of 500 points in which we use the initial conditions

$$u(x) = u_0 - 2u_0\Theta(x - 250),$$

and

$$v(x) = v_0 - 2v_0\Theta(x - 250),$$

where $\Theta(x)$ is the Heaviside function, u_0 is given by Eq. 4 and v_0 is given by Eq. 3.

For the sake of definiteness we fix the values $h = -2.5$, $f = 0.75$ and $g = 0.165$ in order to be in region 2 of Fig. 1. The parameter η sets the spatial scale, and then it has to be chosen in such a way that the profile of the transition contains a sufficient number of points to give the correct shape. With the value chosen there are at least 60 points. The calculation was made using a simple Euler method with a time step of $\Delta t = 0.0012$ and zero flux boundary conditions. The system converges rapidly to a kink in the center that is not moving.

In Fig. 3 we show the numerical results. Observe the peculiar shape of the profile, which is perfectly symmetric in the sense that the area under any of the curves is exactly zero. Observe that the interfaces have a peculiar shape very similar to the ones observed in Fig. 1 of [7], namely

$$u = u_0 \tanh(kx) + a\sin(qx)e^{-p|x|}. \tag{13}$$

If we use the values $a = -0.228$, $k = 0.1705$, $q = 0.1288$ and $p = 0.1345$, the shape of our profile fits this form, indicating that the profile oscillates in the same fashion as proposed by Coullet et al. [7], where the defects present damped oscillatory tails leading to an interacting force. Observe that q and p should be equal to the imaginary and real parts of λ in Eq. 10.

However, if we introduce a small amount of noise, the profile becomes unsymmetrical, and the front acquires a constant velocity. At the edges of the domain, the kink is reflected, due to the zero flux boundary conditions.

In Fig. 4 we show the shape of the profile in the (u, v) plane. The symmetric kink corresponds to the central curve passing through the origin of the (u, v) space. This shape is unstable under small random perturbations. The other two

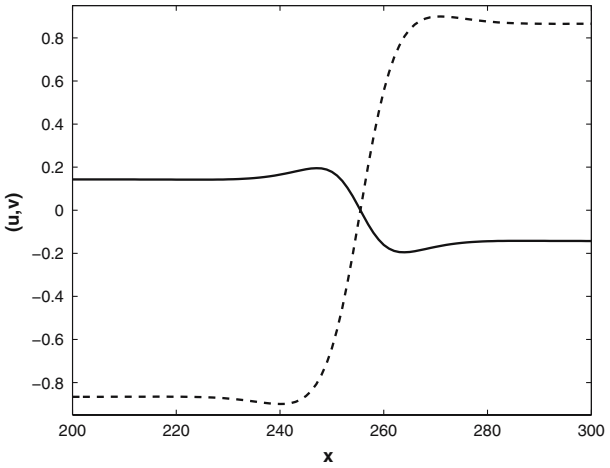

Fig. 3 One-dimensional profile obtained with $f = 0.75$, $g = 0.165$, $D = 1$, and $\eta = 1/12$. This corresponds to region 2 of Fig. 1. The *dashed line* corresponds to v

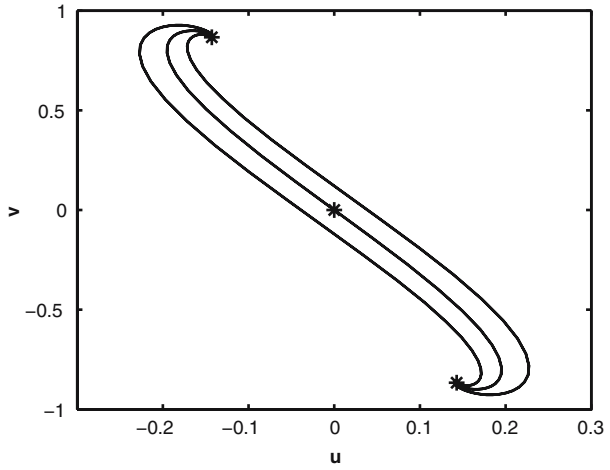

Fig. 4 Form of the possible profiles of the solitary wave solutions in the plane (u, v). The symmetric stationary profile is the central curve passing through the origin. This profile is unstable. The curve on the left corresponds to a form that has an overall negative integral, and the one to the right has positive integral. The sign of the velocity of the wave is opposite for kinks and anti-kinks

curves correspond to the stable asymmetrical profiles. If we define a "kink" as the profile that increases u from left to right, and anti-kink the opposite, one sees that both could travel to the right or to the left. According to Eq. 12 one notices that if the area under the curve is negative for a kink, then the velocity is positive and the kink moves to the right. It is the opposite for the anti-kink. Therefore one could have kinks and anti-kinks traveling in both directions.

In order to illustrate these facts in Fig. 5 we show a calculation using periodic boundary conditions and initiating it with a sine wave profile such that

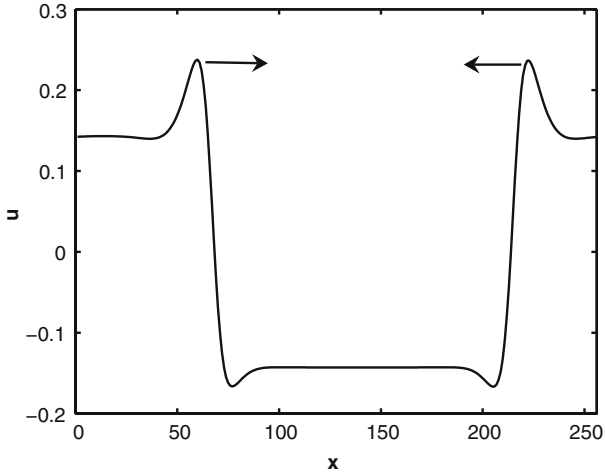

Fig. 5 A kink and an anti-kink colliding. As this calculation is done using periodic boundary conditions, the two excitations circulate forever in opposite directions. Observe that the integral of both profiles is positive. The parameters are the same as in Fig. 3, and the shape of the profile corresponds to the right hand side curve of Fig. 4

it produces a pair kink anti-kink. A small deviation of 10% is introduced in the initial conditions in order to destabilize the symmetric profile and allow the system to find the asymmetric shapes. Observe that if the integral of both profiles is negative, then they move in opposite directions and collide. After the collision the asymmetry is changed.

Numerical calculations with periodic boundary conditions show that a pair of kinks can circulate in the domain forever. However, there is an interesting phenomenon, if one initiates the calculations with random values around $(u, v) = (0, 0)$, a large number of kinks is formed, and once the proper asymmetric form is acquired, they start moving in both directions. It is observed that if the separation of a pair of kinks in less than a certain number ($x \sim 80$ for $\eta = 1/12$) the pair is annihilated when they collide, regardless of the sign of the kinks. At the end one has only the number of kinks and anti-kinks that is allowed by the scale governing the separation of them, some traveling to the right and the rest traveling to the left.

In Fig. 6 we show a typical calculation of this sort. There is definitely a scale governing the pattern. The kinks have properties that identify them as soliton excitations. Once the scale of the system is settled, there are no more annihilations and the number of solitons is conserved. When two of them meet, the kink traveling to the right becomes an anti-kink traveling to the right, and the same happens to the other. The important feature here is that one is able to attain a pattern that is periodic in time. The velocity in this case is 0.1429 (grid length over time units) and the pattern is repeated after a kink has traveled three times the entire domain.

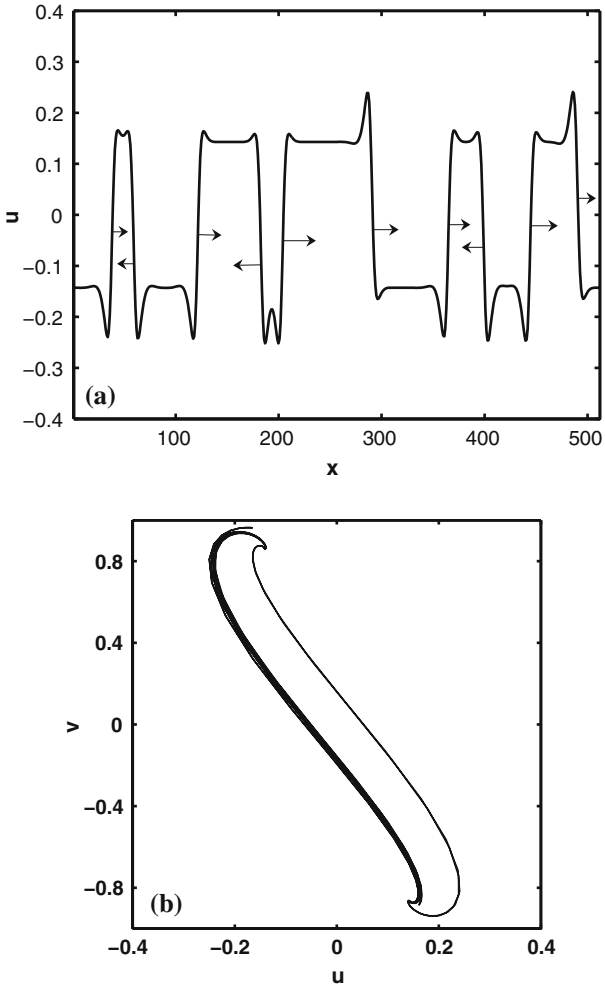

Fig. 6 **a** Profile obtained in a calculation with periodic boundary conditions and random initial conditions, and after 12,300,000 iterations using a time step of $\Delta t = 0.0004$. The scale parameter was $\eta = 1/4$, and all the other parameters are as in Fig. 3. The *arrows* show the direction of the velocity for each kink. Notice that the number of kinks matches the one allowed by the predicted scale of $80/\sqrt{3}$. **b** Plot of the profile in the (u, v) plane of the numerical calculation shown in **a**. Observe that there are more profiles with negative integral, corresponding to the curves on the left

The velocity of the solitary waves depends on the shape of the profile, as we already said. However, it is possible to arrest it if the ratio of diffusion coefficients is not one. We examined this by performing numerical calculations and found that the fronts become stationary for $D < D_c = 0.9$. The transition is second order and the order parameter (which could be the separation between the profile curves in Fig. 4) goes to zero as $(D - D_c)^{1/2}$. This is understood from Eq. 10, which predicts that the velocity c should go as the square root of $(D+1)$.

Another way of arresting the front is to vary f. A numerical calculation with zero flux boundary conditions was made and it was found that the front attains zero velocity at a value $f_c = 0.82$. The velocity approaches zero following the relation $v = (f - f_c)^{1/2}$. It was also seen that for values of $f < 0.74$ the fronts do not bounce at the boundaries of the domain, and the whole systems end up in a uniform value given by one of the fixed points.

Another interesting feature is found if one performs a numerical simulation of a kink moving in a domain which presents a sudden change in the diffusion coefficients. This represents the refraction of the wave front when the properties of the medium in which it travels change. Care has to be taken, since now the correct form of the diffusion terms in Eq. 1 should be $\nabla(\delta D) \cdot \nabla(u)$ and $\nabla(\delta) \cdot \nabla(u)$. There are three regimes of behaviour, depending on the difference of diffusion coefficients ratio in the two sections of the domain. If this difference is not large ($D_1 = qD_2$, with $1 \leq q \leq 1.7266$), the soliton starting from the left, where the diffusion coefficient D_1 is larger, arrives to the border and continues traveling to the right with a smaller velocity, then reaches the edge of the domain and bounces there, as the boundary conditions are zero-flux. When it arrives again to the left part of the domain, it changes its velocity to the corresponding value. If the difference is larger ($1.766 < q \leq 1.8044$), then it arrives again to the interface and diminishes its velocity even more, but now after bouncing in the wall and arriving to the interface again, it is reflected, so it continues bouncing between the right wall and the interface, and never goes back to the region with larger diffusion coefficient. Finally, if the difference between media is extremely large ($q > 1.8044$), the soliton is trapped in the right hand side of the interface after bouncing on the right wall. This picture matches studies of Turing patterns in domains with different diffusion coefficients [11], that show that the transition of the Turing pattern in the interface can be continuous, discontinuous or abrupt, depending on the mismatch between the regions.

In two dimensions the dynamics of the wave fronts is more complicated. It has been pointed out that the velocity of the front depends on the curvature of the profile. This can be investigated in one dimension, assuming that one has initially a circular front with radius r_0 in two dimensions. The velocity, being perpendicular to the front, depends only on the radius $r(t)$. For large radii it has been suggested [12] that the dependence of the velocity on the curvature is linear to an excellent approximation, in our case this means that

$$\frac{dr}{dt} = c_0 - \frac{\kappa}{r}, \tag{14}$$

where c_0 is the velocity of a planar front, and κ is a positive constant. Observe that the velocity is larger when the front is concave that when it is convex. Integrating Eq. 14 one obtains

$$t = \frac{r - r_0}{c_0} + \frac{\kappa}{c_0^2} \ln \frac{c_0 r - \kappa}{c_0 r_0 - \kappa}. \tag{15}$$

We have performed numerical calculations for $f = 0.65$ and $\eta = 1/12$ and found that $\kappa = 1.002$ and $c_0 = 0.146$ for large radii. As the wave front velocity varies with the curvature of the profile, we expect that in a calculation in a 2D domain, the concave structures tend to disappear, while the convex regions dominate.

2.2 Dynamics in two dimensions

In the border between regions 2 and 5 of the phase diagram (Fig. 1), the limit cycle still persists, meaning that one could find oscillatory solutions in two dimensions. In Fig. 7a we show a snapshot of a pattern generated in this region by setting equal values of the diffusion coefficients ($D = 1$) in Eq. 2. The calculation was started with random initial conditions around the $(0, 0)$ fixed point, and periodic boundary conditions. In Fig. 7b the values of the points in the 256×256 grid are plotted. Observe that the points tend to travel from the center to the limit cycle, indicated by the continuous line. This oscillating pattern resembles the familiar pattern in the Belousov–Zhabotinskii reaction, namely gyrating spirals of a given size. The temporal behavior is plotted in Fig. 7c where the

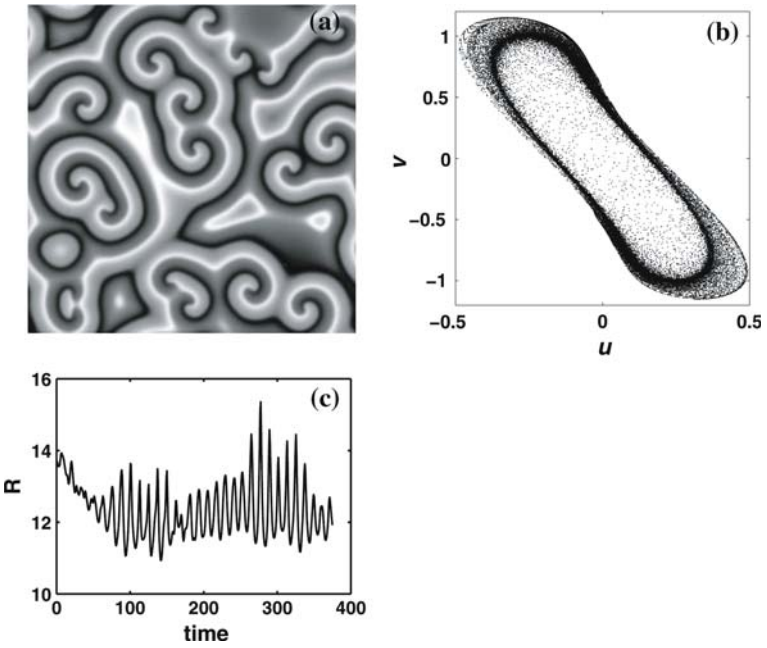

Fig. 7 **a** Pattern obtained for parameters precisely on the border of regions 2 and 5 of Fig. 1, after 500,000 iterations. The values are $g = 0.165$, $h = -2.5$, and the critical value $f_c = 0.5043$. **b** The values of (u, v) for each point at a fixed time are displayed as dots. As time runs these points tend to approach the limit cycle also shown as a continuous line. **c** Plot of R versus time (in dimensionless units), this quantity is the first zero of the pair correlation function averaged over all angles, and $dt = 0.002$

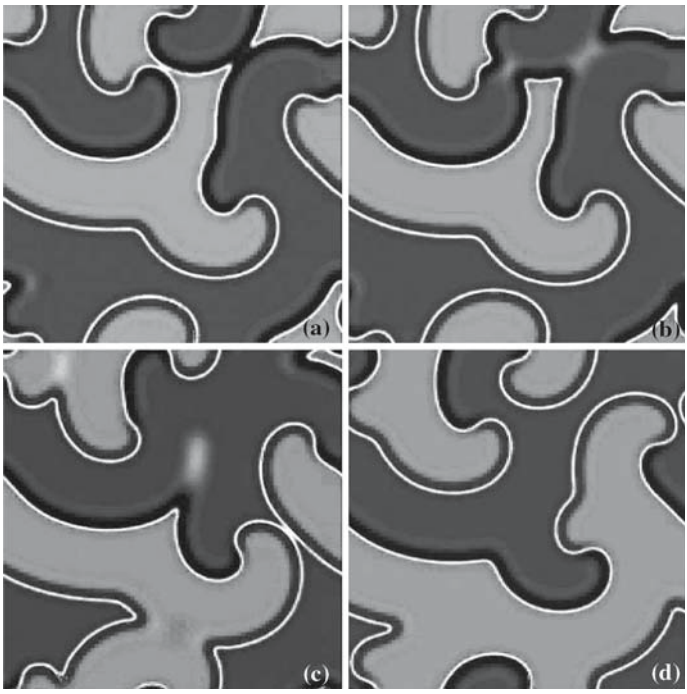

Fig. 8 Four snapshots of a pattern consisting of solitary wave fronts. Observe the appearance of a characteristic length and the peculiar way in which the pattern moves. One can detect points that do not move and the fronts rotate around them, giving the impression of spiral wave. This pattern resembles very much the behaviour of miocardial waves

parameter R measures the size of the patterns formed. This R is the first zero of the pair correlation function, averaged over angle and calculated numerically at all times. Observe the oscillatory behavior of the graph.

These spiral waves seem to be ubiquitous in many non-linear systems [12] ranging from models without diffusion to the Kuramoto equations with equal diffusion coefficients, and Brusselator models with complex amplitudes. Our model captures these solutions as well.

Now, we shall examine the appearance of solitary waves in two dimensions. We choose the same region in phase space as for our studies in one dimension of the previous section.

In Fig. 8 we show a calculation made using the same parameters as in Fig. 2d, that is, in region 2 of the phase diagram, just avoiding the presence of the limit cycle. The spatial scale of the figure is $\eta = 1/2$. Observe that the velocity of the fronts depends on the curvature of the profile, therefore the fronts acquire a sort of rotation around certain points that do not move. This behavior could be mistaken by a pattern of spiral waves, as in Fig. 7, but it is not. The size of the domain contains 256 points per side. The calculation was initiated with random initial conditions and a number of fronts are annihilated before it settles to a given scale, in this case one can see that the scale is approximately

Fig. 9 Pattern obtained with $g = 0.165$, $h = -2.5$, $f = 0.75$, and for $D = 0.8$, after 500,000 iterations in a square grid of 256 points per side. With these parameters, there is no limit cycle in the absence of diffusion. The *inset* shows the power spectrum of the pattern

50 pixels. After 300,000 iterations the pattern converges to a steady oscillatory state. This corresponds to 300 time units. The period of oscillation was measured by calculating the first zero of the correlation function, and it was found to be approximately 75 time units. The four snap shots in the figure correspond roughly to a time span of 12 units.

In one dimension we have seen that a difference in the diffusion constants locks the wave fronts in space, obtaining a spatial pattern that resembles spatial chaos, although we know that this is not so, since there is a well determined scale. We expect that a stationary spatial pattern is obtained also in two dimensions.

In Fig. 9 we show a pattern generated with random initial conditions around the point $(0, 0)$. The diffusion coefficient ratio is now $D = 0.8$, predictably a value in which the pattern gets locked. The pattern is extremely stable in space and represents the 2D version of the "spatial chaos" found in the previous section. Observe that, contrary to the 1D case, the pattern does not get locked in a position with many separation distances between stripes, but finds a way to accommodate the stripes in an orderly manner. Observe the power spectrum shown in the inset that clearly exhibits a ring at a definite value of k vector. This further demonstrates the existence of a fixed scale in the problem.

3 Discussion and conclusions

We have examined the dynamics of wave fronts in one and two dimensions. Our analysis in one dimension reveals that there is a region of parameters in which solitons travel with constant velocity and collide in a normal fashion when the density of them corresponds to a given spatial scale. If this density is larger, collisions between fronts result in pair annihilation. When one uses a domain with periodic boundary conditions, a periodic pattern of traveling fronts sets in, consisting of solitons moving to the right and left forever. With zero-flux boundary conditions the solitons reflect at the boundaries, and collide maintaining their constant velocity.

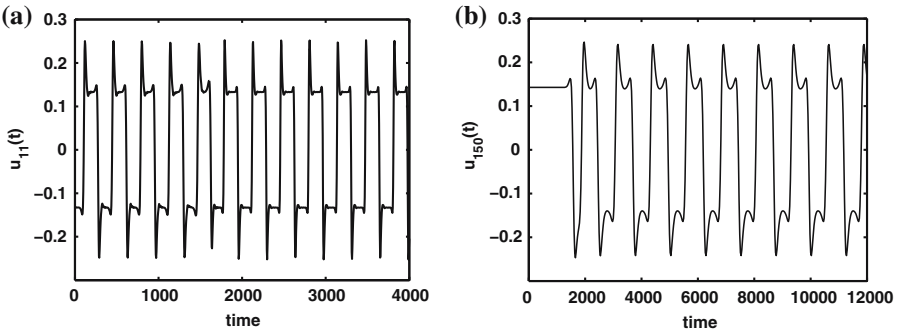

Fig. 10 **a** Time history of the field u in Fig. 8 calculated at the point (1,1). The time scale is in normalized units. **b** Time history of u for the central point of a 1D domain, the parameters are the same as in Fig. 6

The velocity depends on the values of both the diffusion coefficients ratio (D), and on the parameters (f, g, h). We showed that the velocity of the fronts becomes zero as a second order phase transition with D and f as order parameters. The velocity goes to zero as a power law with exponent 1/2 in both cases. This exponent is the same as the one found in the analysis of the simple Fisher equation [12], and it is also the mean field value. As a consequence of the dependence of the velocity on D, the fronts may refract at the interface between two regions with different diffusion properties. We found numerically that the solitons could be trapped in the region of smaller D, or even stop at the interface.

In two dimensions these results can be found as well, but the dynamics is richer, since it is found that the velocity depends on the local curvature of the front. This can be demonstrated with a calculation in one dimension in polar coordinates, that simulates the growing of a circular front in two dimensions. This feature produces the interesting shapes of Fig. 8, which shows a pattern of moving solitons that conserves a spatial scale and that is periodic in time, with certain stationary points that are the pivots of rotational motion. This dynamics resembles the waves measured in cardiac tissue [13], and makes our model ideal to be applied to this kind of studies.

In modeling the dynamics of the heart beat with PDF, one usually chooses the kinetics as simple as possible, and still retaining the basic non-linear properties measured in experiment, as the existence of limit cycles, double period bifurcations, and spiral wave dynamics. These features are present in the simple Fitzhugh–Nagumo equations, which bears the general form of our model. Much work has been done in this direction and an exhaustive study of spiral waves in this model exists [8]. However, we want to point out that the waves found in experiments resemble more the dynamics of our soliton pattern of Fig. 8. We also believe that these kind of wave fronts are more realistic for the representation of models of axon conduction, and are less complicated than the biologically based models, and more useful than the cable models. In order to support this claim, in Fig. 10a we show the time history of the point (1,1)

in the calculation of Fig. 8. Observe the peculiar shape of the oscillations, that resemble some of the waves measured in electrocardiograms.

In one dimension it is difficult to get a periodic time history from a random pattern. We produced a periodic train of solitons in a domain with zero flux boundary conditions, by starting with a single soliton on the left and changing the sign of u every 684 time units. This choice produces a separation between solitons that is shorter than the scale, therefore the solitons that bounce on the right wall are annihilated by the ones coming from the left. The results for the time history of the u at the central point $N = 150$ are shown in Fig. 10b. Observe that the wave shape is very similar to the 2D calculation.

One usually models complex behaviour of oscillating patterns with cellular automata [5], due to the fact that ODE models are cumbersome numerically. At present we are studying the possibilities of transitions between the perfect periodic oscillating pattern of solitons and other non-periodic patterns.

To summarize, in this paper we have examined a reaction diffusion model in conditions such that it presents three fixed points. This allows the study of a situation in which one has two stable fixed points and one unstable one, or a bistable system. We found solitary waves that move with a given velocity. This richness of behavior makes models like this very useful in applications, and allow us to get insight into the mechanisms of pattern formation and selection in a wide variety of interesting problems.

Acknowledgments R.A.B. is grateful to the Laboratory of Computational Engineering for an adjunct professorship. Financial support from project F-40615 from CONACyT is also acknowledged.

References

1. Aragón, J.L., Varea, C., Barrio, R.A., Maini, P.K.: FORMA **13**, 154 (1998)
2. Aragón, J.L., Torres, M., Gil, D., Barrio, R.A., Maini, P.K.: Phys. Rev. E **65**, 051913 (2002)
3. Barrio, R.A., Varea, C., Aragón, J.L., Maini, P.K.: Bull. Math. Biol. **61**, 483 (1999)
4. Bray, A.J.: Adv Phys **43**, 357 (1994)
5. Bub, G., Shrier, A., Glass, L.: Phys. Rev. Lett. **88**, 058101 (2002)
6. Castets, V., Dulos, E., Boissonade, J., Kepper, P.D.: Phys. Rev. Lett. **64**, 2953 (1990)
7. Coullet, P., Elphick, C., Repaux, D.: Phys. Rev. Lett. **58**, 431 (1987)
8. Davidsen, J., Glass, L., Kapral, R.: Phys. Rev. E **70**, 056203 (2004)
9. Leppänen, T.: Computational studies of pattern formation in Turing systems. Ph.D. thesis, Helsinki University of Technology (2004), and in current topics in physics. In: Barrio, R.A., Kaski, K.K., (eds.) Imperial College Press 199 (2005)
10. Liaw, S.S., Yang, C.C., Liu, R.T., Hong, J.T.: Phys. Rev. E **64**, 041909 (2001)
11. Maini, P.K., Benson, D.L., Sherratt, J.A.: IMA J. Math. Appl. Med. Biol. **9**, 197 (1992)
12. Murray, J.D.: Mathematical biology II: spatial models and biomedical applications. Springer, Berlin (2003)
13. Nagai, Y., González, H., Shrier, A., Glass, L.: Phys. Rev. Lett. **84**, 4248 (2000)
14. Plaza, R., Sanchez-Garduño, F., Padilla, P., Barrio, R.A., Maini, P.K.: J. Dyn. Differ. Equ. **16**, 1093 (2004)
15. Rabinovich, M.I., Ezersky, A.B., Weidman, P.D.: The Dynamics of Patterns. World Scientific, London (2000)
16. Turing, A.M.: Phil. Trans. R. Soc. Lond. B **237**, 37 (1952)
17. Yang, L., Epstein, I.R.: Phys. Rev. Lett. **90**, 178303 (2003)